PNAS RESEARCH ARTICLE | PHARMACOLOGY

Persistent binding at dopamine transporters determines sustained psychostimulant effects

Marco Niello[a,1], Spyridon Sideromenos[b], Ralph Gradisch[a], Ronan O´Shea[c], Jakob Schwazer[a], Julian Maier[a], Nina Kastner[a], Walter Sandtner[a], Kathrin Jäntsch[a], Carl R. Lupica[c], Alexander F. Hoffman[c], Gert Lubec[d], Claus J. Loland[e], Thomas Stockner[a], Daniela D. Pollak[b], Michael H. Baumann[f], and Harald H. Sitte[a,g,1]

Edited by Donald Pfaff, Rockefeller University, New York, NY; received August 2, 2021; accepted December 28, 2022

Psychostimulants interacting with the dopamine transporter (DAT) can be used illicitly or for the treatment of specific neuropsychiatric disorders. However, they can also produce severe and persistent adverse events. Often, their pharmacological properties in vitro do not fully correlate to their pharmacological profile in vivo. Here, we investigated the pharmacological effects of enantiomers of pyrovalerone, α-pyrrolidinovalerophenone, and 3,4-methylenedioxypyrovalerone as compared to the traditional psychostimulants cocaine and methylphenidate, using a variety of in vitro, computational, and in vivo approaches. We found that in vitro drug-binding kinetics at DAT correlate with the time-course of in vivo psychostimulant action in mice. In particular, a slow dissociation (i.e., slow k_{off}) of *S*-enantiomers of pyrovalerone analogs from DAT predicts their more persistent in vivo effects when compared to cocaine and methylphenidate. Overall, our findings highlight the critical importance of drug-binding kinetics at DAT for determining the in vivo profile of effects produced by psychostimulant drugs.

dopamine transporter | drug-binding kinetics | psychostimulants | cathinones | new psychoactive substances

Significance

The investigation of DAT ligands in vitro is typically assessed at thermodynamic equilibrium, which may not mimic the complex physiological conditions in vivo. Here we demonstrate that various DAT inhibitors can be distinguished based on their in vitro binding kinetics, and that the in vitro k_{off} of a drug at DAT correlates with the duration of in vivo psychostimulant effects in mice. We show that the *S*-enantiomers of pyrovalerone and its analogs, αPVP, and MDPV, display slow in vitro kinetics at DAT and long-lasting psychostimulant effects, which differs from the fast in vitro kinetics and short-lasting effects of drugs like cocaine. Our study provides key evidence that binding kinetics at DAT is an important determinant of psychostimulant drug action.

The dopamine transporter (DAT) is a neuronal membrane protein that retrieves previously released dopamine from the extracellular space and moves it back into presynaptic nerve terminals (1). The importance of DAT in the regulation of brain dopaminergic signaling is well established based on decades of in vitro and in vivo experimental evidence (2–6). From a clinical perspective, single-point mutations altering DAT function are associated with a variety of psychiatric disorders, highlighting the importance of DAT in normal and pathological conditions (7–9). Compounds targeting DAT, and other monoamine transporters (MATs), are classified as inhibitors if they bind to the transporter and prevent neurotransmitter uptake, or as releasers if they act as substrates and reverse the normal direction of transporter flux (10). Regardless of their mechanism of action as inhibitor or releaser, drugs which interact more potently at DAT compared to the serotonin transporter (SERT) are typically associated with a higher abuse potential (11–13). Therefore, the DAT/SERT selectivity ratio is regularly used to predict the abuse liability of transporter ligands (14). However, cocaine, despite showing an unselective DAT/SERT profile, still shows high abuse liability. Similarly, several benztropines, which instead possess high DAT selectivity, do not possess pronounced reinforcing properties. The case of cocaine and benztropines suggest that while the DAT/SERT ratio is still an important tool for general toxicological predictions, it does not always hold true, and it highlights a fundamental gap in our understanding of psychostimulants mechanism of action (15). As a matter of fact, in addition to the fundamental inhibitor/releaser distinction, an emerging complexity for transporter pharmacology has been recently realized with the discovery of partial releasers (16), allosteric inhibitors (17), and atypical transporter ligands (15).

New psychoactive substances (NPS) are synthetic versions of drugs of abuse which are specifically engineered to bypass current drug control laws (18), and synthetic cathinones represent a major class of stimulant-like NPS (19). One group of synthetic cathinones are pyrovalerone analogs, such as α-pyrrolidinovalerophenone (αPVP) and 3,4-methylenedioxypyrovalerone (MDPV), which display high-affinity binding to DAT (20) and prolonged stimulatory effects in humans (21–25). The molecular basis for the prolonged effects of pyrovalerone analogs is currently unknown. Some studies suggest that phase I metabolites might play a role in synthetic cathinone pharmacology (26, 27), but it is unclear whether pharmacodynamic processes, rather than bioactive metabolites, would influence the acute effects of pyrovalerone analogs. Studying their molecular mechanism of action might unveil pharmacodynamic parameters involved in psychostimulant activity.

Both MDPV and αPVP are high-affinity inhibitors of DAT and the norepinephrine transporter (NET) but devoid of significant activity at SERT (27–29). The illicit use of both

Author contributions: M.N., W.S., T.S., and H.H.S. designed research; M.N., S.S., R.G., R.O., J.S., J.M., N.K., W.S., K.J., A.F.H., C.J.L., and M.H.B. performed research; C.L., G.L., T.S., D.D.P., and H.H.S. contributed new reagents/analytic tools; M.N., S.S., R.G., R.O., J.S., J.M., N.K., W.S., K.J., A.F.H., C.J.L., C.R.L.,T.S., and M.H.B. analyzed data; M.N. interpreted the data; and M.N., M.H.B., and H.H.S. wrote the paper.

The authors declare no competing interest.

This article is a PNAS Direct Submission.

[1]To whom correspondence may be addressed. Email: marco.niello@meduniwien.ac.at or harald.sitte@meduniwien.ac.at.

This article contains supporting information online at https://www.pnas.org/lookup/suppl/doi:10.1073/pnas.2114204120/-/DCSupplemental.

Published February 2, 2023.

αPVP and MDPV in humans induces psychostimulant effects and can cause severe adverse effects including delusions, paranoia, hallucinations, and cardiovascular collapse (23–25, 30). Importantly, their pharmacological effects occur within 10 min after administration of a single dose (15 to 100 mg) and can last for multiple hours (23, 31). A study in humans found that αPVP could still be detected in the bloodstream 6 h after nasal insufflation and 20 h after rectal administration (32), and psychotic episodes have been reported as long as 6 d after consumption (22). The sustained clinical effects of αPVP and MDPV differ substantially from traditional DAT inhibitors like cocaine, which has a similar onset of action to αPVP and MDPV but much shorter duration of effects (33–35). While αPVP and MDPV are both used rarely among young people (1% of high school in United States; (36, 37)), consumption of the drugs at their peak in popularity led to thousands of emergency departments visits and many deaths in the United States (36, 37). Moreover, new analogs of αPVP continue to emerge in clandestine drug markets worldwide (e.g., α-pyrrolidinohexiophenone or αPHP), presenting a public health threat (38, 39).

Preclinical studies investigating the effects of αPVP in rodents demonstrate avid self-administration (13, 40) and robust place preference (41), together with prolonged stimulatory effects on locomotion (42), blood pressure, and heart rate (28). While αPVP self-administration and conditioned place preference are related to drug activity at DAT, increases in blood pressure and heart rate most likely involve drug activity at NET. αPVP possesses a single chiral center, meaning that it exists as two different enantiomers, the *R*- and *S*-isomers. In general, enantiomers have identical physicochemical properties but a different three-dimensional orientation of the functional groups bound to the chiral carbon, which can confer pronounced differences in pharmacology (43).

Based on preclinical studies with αPVP, and previous findings of cathinone enantioselectivity at MATs (28, 44–47), we decided to use αPVP enantiomers as tools to determine whether interactions at DAT might underlie the sustained time-course of drug actions. Given the established role of DAT in psychomotor processes (4, 15) and our interest in the respective psychostimulant effects, we have focused our research on DAT and left the activity at NET to future investigations.

In the present study, we first investigated the interactions of αPVP enantiomers with DAT as compared to the effects of cocaine based on the observation of a significantly extended effect duration when compared to cocaine (22, 23, 31, 32). We found that i) the *S*-isomer of αPVP displays much greater affinity for DAT when compared to the *R*-enantiomer; ii) both enantiomers of αPVP display a time-dependent, non-competitive pharmacology upon interaction with DAT; and iii) the non-competitive pharmacology relies on a slow dissociation rate at DAT, with slower dissociation rates for αPVP enantiomers when compared to cocaine. Lastly, we expanded our in vitro and in vivo analysis to include enantiomers of other DAT inhibitors, as well as the clinically used methylphenidate (MPH), to show that slow dissociation rate from DAT is highly correlated with persistent psychostimulant effects of *S*-pyrovalerone, *S*-αPVP, and *S*-MDPV in mice. Overall, our results demonstrate that binding kinetics represent an important property of DAT inhibitors that can impact psychostimulant action and need to be investigated in particular when exploring novel therapeutic options for neuropsychiatric disorders.

Results

αPVP Enantiomers Are Stereoselective Non-Competitive Inhibitors at DAT. For our initial experiments, we examined the ability of αPVP isomers (*SI Appendix*, Fig. S1*A*) to act as inhibitors or substrates at DAT. In uptake inhibition assays carried out in HEK293 cells stably expressing DAT, *S*-αPVP was 125-fold more potent (IC_{50} = 0.02 μM) than *R*-αPVP (IC_{50} = 2.5 μM) and 25-fold more potent than cocaine (IC_{50} = 0.51 μM). Both αPVP enantiomers were essentially ineffective at inhibiting SERT (*S*-αPVP IC_{50} = 207 μM; *R*-αPVP IC_{50} = 628 μM) and showed no evidence of enantioselectivity in this regard (*SI Appendix*, Fig. S1 *B* and *C*). It is well established that DAT substrates induce transporter-mediated inward Na^+ currents. In an electrophysiological examination of DAT-mediated currents, we found that the cognate substrate dopamine (DA) produced robust inward currents, whereas neither of the αPVP enantiomers did. In sum, our initial results confirm that *S*- and *R*-αPVP are enantioselective DAT inhibitors with no measurable substrate activity (*SI Appendix*, Fig. S1 *D–F*).

To evaluate whether the DAT binding profile determined in transfected cells is translated to DAT function in native tissue preparations, we evaluated the effects of αPVP enantiomers and cocaine on inhibition of [^{3}H]DA uptake in rat striatal synaptosomes. In agreement with data from HEK293 cells, *S*-αPVP was a more potent inhibitor of uptake (*S*-αPVP IC_{50} = 6.9 nM) than either cocaine (IC_{50} = 255.2 nM) or *R*-αPVP (IC_{50} = 306.8 nM) in rat striatum (*SI Appendix*, Fig. S2*A*). In synaptosomes, we found cocaine and *R*-αPVP to be nearly equipotent at inhibiting uptake, whereas in HEK293 cells, cocaine was more potent. Next, we assessed the ability of the drugs to inhibit DAT in an intact tissue preparation using fast scan cyclic voltammetry (FSCV) in rat striatal slices (*SI Appendix*, Fig. S2*B*). Consistent with DAT binding and uptake inhibition results, *S*-αPVP was a more potent inhibitor (IC_{50} = 136 nM) of DA clearance when compared to *R*-αPVP (IC_{50} = 776 nM) and cocaine (IC_{50} = 5,535 nM; *SI Appendix*, Fig. S2*C*). In the FSCV assay, the potency of *R*-αPVP to inhibit DA clearance was left-shifted compared to cocaine. In general, the data from the rat synaptosome and rat slice experiments agree that *S*-αPVP is more potent at inhibiting DA clearance and uptake when compared to *R*-αPVP and cocaine, though there were differences in absolute and relative potencies of the drugs across the two assays.

Next, we examined the nature of the interaction between αPVP enantiomers and DAT. More specifically, we wished to examine whether αPVP isomers inhibit DAT by a competitive mechanism, similar to cocaine (48), or by a non-competitive mechanism. Previous work shows that cocaine binds to the orthosteric S1 site on DAT, thereby competing with the endogenous substrate dopamine for this site (49, 50). Data depicted in Fig. 1 confirm that cocaine interacts with DAT in a competitive manner, with a concentration-dependent increase in K_m but no change in V_{max} for [^{3}H]DA uptake (Fig. 1 *A–C*). By contrast, in the case of the *S*- and *R*-enantiomers of αPVP, we found concentration-dependent decreases in V_{max} without major changes in K_m (Fig. 1 *D–F* and *G–I*, respectively). The reduction in the V_{max} is not mediated by a reduction in DAT expression (*SI Appendix*, Fig. S3), thereby suggesting a non-competitive mechanism of action. Non-competitive inhibition of transporters has been previously reported in the case of allosteric and atypical inhibitors (17, 51).

S-αPVP Occupies the S1 Orthosteric Site of DAT. Both allosteric and atypical inhibitors can show non-competitive pharmacology. In the case of allosteric modulators, non-competitive action is due to the presence of a secondary binding site (S2) in the target protein that can modify the response of the orthosteric binding site (*SI Appendix*, Fig. S1 and Fig. 2 *A*, *Top Right*). By contrast, atypical inhibitors interact with the orthosteric binding site, but they elicit a conformational rearrangement which prevents further competitive binding (Fig. 2 *A*, *Bottom Right*). To further elucidate

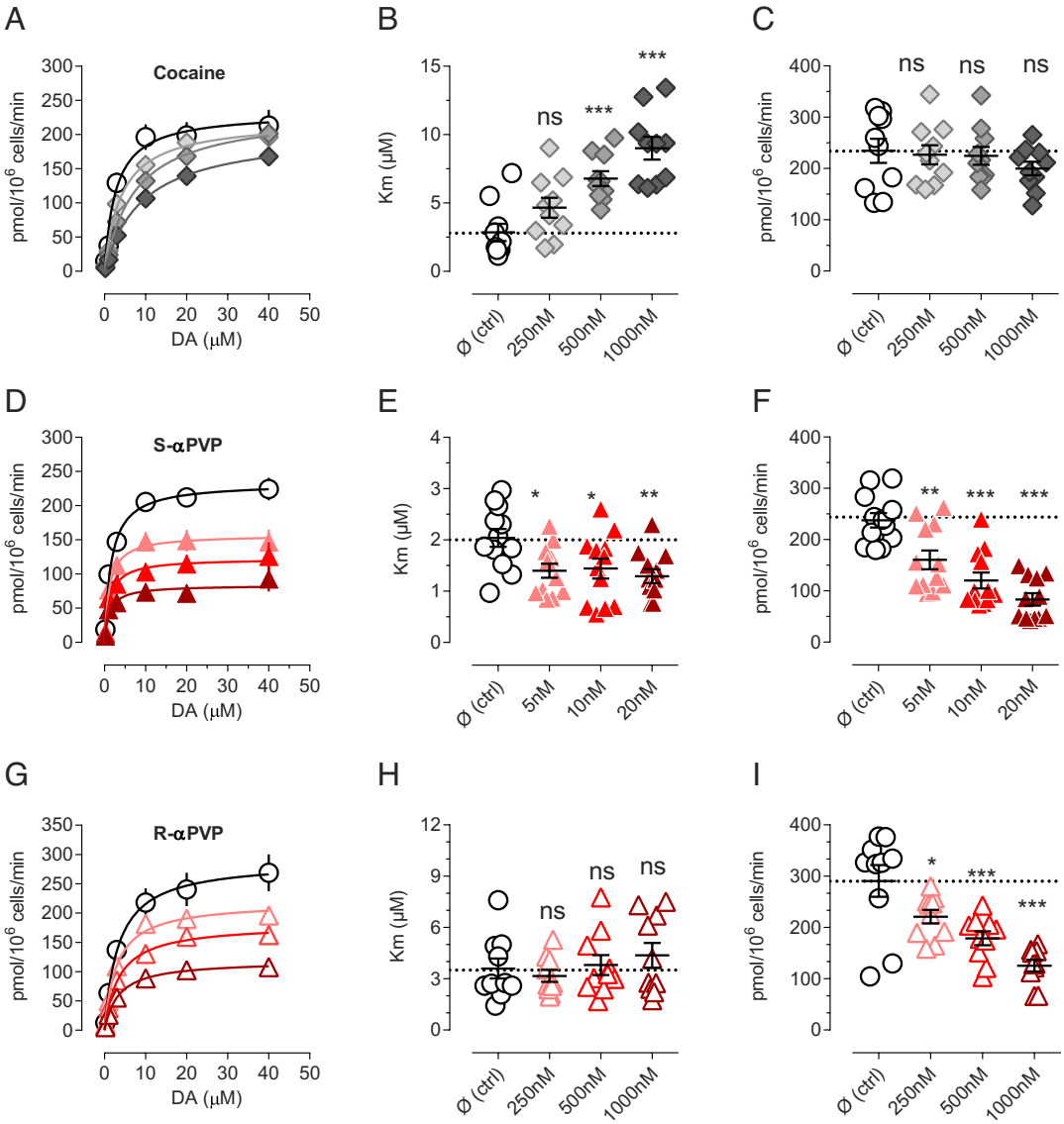

Fig. 1. Non-competitive inhibition of αPVP enantiomers. (*A*) Saturation of DA uptake conducted in the presence of cocaine 250 nM (light gray), 500 nM (gray), or 1,000 nM (dark gray). (*B*) Cocaine increases K_m in dose-dependent manner but (*C*) does not decrease V_{max}. (*D*) Saturation of DA uptake conducted in the presence of S-αPVP 5 nM (light red), 10 nM (red), or 20 nM (dark red). (*E*) αPVP does not drastically change the K_m, but (*F*) reduces V_{max} dose-dependently. (*G*) Saturation of DA uptake conducted in the presence of R-αPVP 250 nM (light red), 500 nM (red), or 1,000 nM (dark red). (*H*) R-αPVP does not drastically change the K_m, but (*I*) reduces V_{max} dose-dependently. Data are shown as mean ± SEM of at least five independent experiments conducted in duplicates. Statistics is conducted with one-way ANOVA followed by Dunnett's post hoc multiple comparison vs. control (Ø). **=$P < 0.01$, ***$P < 0.001$, ****$P < 0.0001$.

the non-competitive nature of αPVP interactions with DAT, we measured dissociation of the phenyltropane-analogue [^{3}H]WIN35428 from membranes prepared from HEK293 cells over-expressing human DAT. This experiment is based on the notion that allosteric inhibitors attenuate the dissociation of a radioactive tracer pre-bound into the orthosteric site (17). Similar to the effects of cocaine, the fast dissociation rate of [^{3}H]WIN35428 was not affected by the application of αPVP enantiomers (Fig. 2*B*). Since changes to radioligand dissociation rates are dependent on the precise radiotracer employed (52), we also conducted single-point uptake inhibition assays using [^{3}H]DA as the radiotracer. Allosteric inhibitors display a greater degree of inhibition when co-incubated with orthosteric ligands (52). Neither of the αPVP enantiomers showed cooperative inhibition (Fig. 2*C*), excluding the possibility of an allosteric mechanism at DAT.

In an attempt to define specific attributes of the binding site for αPVP enantiomers, we applied site-directed mutagenesis to the DAT central binding site. Given the high DAT/SERT selectivity of αPVP (*SI Appendix*, Fig. S1*B*), we swapped non-conserved residues between the DAT and SERT central binding site and tested their impact on cocaine, *S*-αPVP, and R-αPVP activity in uptake inhibition experiments. Here we converted IC_{50} values into Ki values using the Cheng-Prusoff equation (see *Methods* in the *SI Appendix*), in order to account for the effect of the point mutations on transport efficiency. The K_m value for each mutant is reported in *SI Appendix*, Table S1. As shown in Fig. 2 *D*–*F*, mutation of DAT phenylalanine 76 to a tyrosine residue (i.e., DAT-F76Y) shifted the inhibition curves of αPVP enantiomers to the right, with a sixfold increase in the Ki value when compared to DAT wild-type (WT) (Fig. 2*G*; S-αPVP: Ki for DAT-WT = 0.01 μM vs. Ki for DAT-F76Y = 0.06 μM; R-αPVP: Ki DAT-WT = 0.37 μM vs. Ki DAT-F76Y = 2.19 μM). This same mutation induced no pharmacologically relevant change in the affinity of cocaine for DAT (cocaine: Ki for DAT-WT = 0.20 μM vs. Ki for DAT-F76Y = 0.32 μM). The Ki values obtained for each mutant are reported in *SI Appendix*, Table S2.

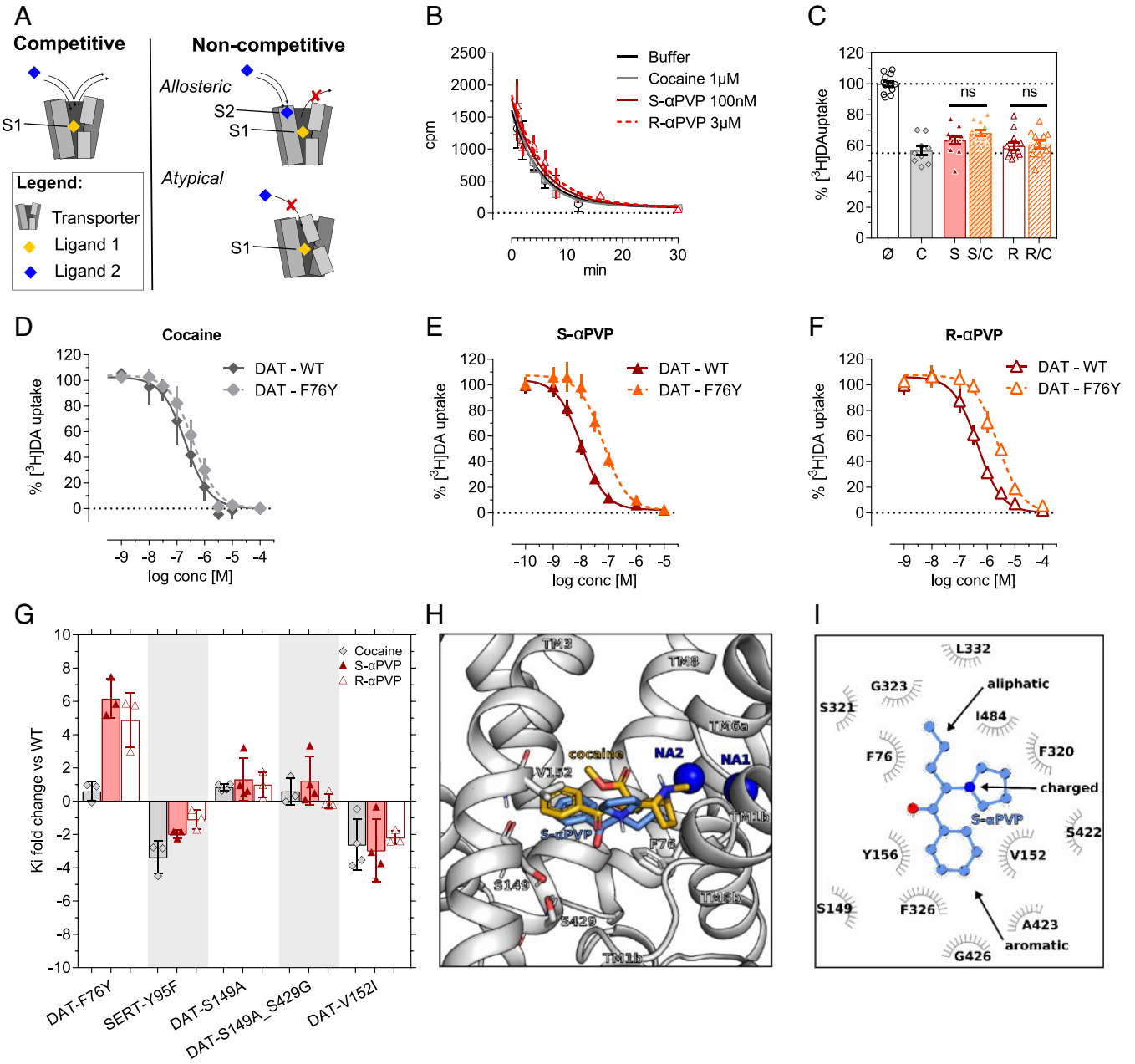

Fig. 2. Cocaine and αPVP enantiomers binding mode in DAT. (*A*) Mechanism of action of competitive and non-competitive (allosteric vs. atypical) inhibition. (*B*) Dissociation of [^{3}H]WIN35428 in DAT membranes. Data are mean ± SEM n ≥ 3 independent experiments conducted in duplicates. (*C*) Single-point uptake inhibition of 0.2 µM [^{3}H]DA conducted in HEK293cells stably expressing DAT. Compounds are pre-incubated at their IC_{50} alone or in combinations (Ø =control, untreated; C = cocaine 100 nM; S = S-αPVP 10 nM; S/C = cocaine 100 nM + S-αPVP 10 nM; R = R-αPVP 300 nM; R/C = R-αPVP 300 nM + cocaine 100 nM). One-way ANOVA followed by Dunnett´s multiple comparison test vs. cocaine *=$P < 0.05$, **=$P < 0.01$, ***=$P < 0.001$. (*C*–*F*) DAT-WT and DAT-F76Y uptake inhibition profiles for cocaine, S-αPVP and R-αPVP. (*G*) Site-directed mutagenesis of DAT orthosteric binding site. DAT residues are mutated in the corresponding residue in SERT. Data are shown as Ki fold change compared to WT DAT (mean ± SD). Every symbol represents an individual experiment conducted in triplicate. (*H*) Membrane and front view of the S1 site of the human DAT showing the best docking pose of S-αPVP (blue) and the binding pose of cocaine elucidated by X-Ray in dDAT (PDB: 4XP4) (orange). TM10 and TM11 are not shown for clarity, while residues F76, S149, V152, and S429 are highlighted as sticks and colored by atom type. The two sodium ions are represented as dark blue spheres. (*I*) 2D interaction map of S-αPVP with the human DAT according to the binding mode shown in panel *H*.

To characterize the precise binding pose of αPVP within the DAT protein, we performed docking experiments of the more potent *S*-isomer using a homology model of the human DAT and compared it to the one of cocaine (*Material and Methods*). The structure of *S*-αPVP can be divided into three structural components: an aromatic ring, an aliphatic tail, and a positively charged nitrogen-containing pyrrolidine ring (Fig. 2*I*). The best docked pose of *S*-αPVP shows that its aromatic ring is located in the S1 binding site between TM3 and TM8 (Fig. 2*H*). The orientation of the aromatic ring is in agreement with the conformations observed for dopamine, amphetamines, and also for inhibitors like cocaine, RTI-55, and nisoxetine (5, 50); however, the overall binding mode of αPVP within the S1 site differs from the one of cocaine, in agreement with our in vitro data. The hydrophobic side chains of DAT-V152 and DAT-Y156 on TM3 and of DAT-A423 on TM8 stabilize the aromatic ring of *S*-αPVP by hydrophobic interactions. The aliphatic tail of *S*-αPVP forms extensive interactions with DAT-F76, which is part of the intracellular hydrophobic gate (Fig. 2*H*). The bulky and positively charged pyrrolidine moiety of *S*-αPVP establishes hydrophobic

interactions with DAT-I484 and DAT-F320; in addition, the charged nitrogen is interacting with the backbone carbonyl group of DAT-F320 on TM6a that carries a negative partial charge. Instead, cocaine interacts differently with SERT due to an overall larger and hence bulkier size, (cocaine = 303.25 g/mol; *S*-αPVP 231.11 g/mol). Similar to *S*-αPVP, the cocaine moiety protrudes between the scaffolds of TM3 and TM8, and the tropane substituent protrudes much deeper between the unwound regions of TM1 and TM6. Thus, cocaine forms a salt bridge with D79 and a hydrogen bond with F320. The overall result is that cocaine is slightly lifted toward the outer vestibule in comparison with *S*-αPVP, thereby being out of the interaction distance with F76. Overall, our in vitro data suggest that despite showing a non-competitive pharmacology, αPVP enantiomers do not interact with the putative allosteric site but rather with the orthosteric site. Importantly, our mutagenesis study identified one crucial residue, DAT-F76 that selectively impairs the interaction of DAT and αPVP enantiomers but not of dopamine and cocaine.

Measuring Off Rates of Unlabeled DAT Inhibitors. To reconcile the surprising fact that αPVP enantiomers display non-competitive pharmacology but still bind within the orthosteric site, we hypothesized that this might be due to slow binding kinetics, as already described in the case of different G-protein coupled receptors (53–55). To evaluate this possibility, we have initially relied on kinetic modeling, using a simplified model of DAT transport cycle that includes an inhibitor-bound state (ToNaI; Fig. 3*A*). Simulations of DAT uptake in the presence of a DAT inhibitor with a slow dissociate constant (k_{off}) of 0.01 s^{-1} showed an apparent non-competitive pharmacology during 1-min uptake incubation time, which is in agreement with our in vitro findings (cft *SI Appendix*, Fig. 4*A* with Fig. 1). Extending the in silico uptake incubation time to 10 min allows drug dissociation and the equilibration of the inhibitor, demonstrating competitive pharmacology (*SI Appendix*, Fig. S4*B*). In vitro uptake experiments with extended uptake time (6 min—for longer time, uptake was deviating from linearity) and confirmed our in silico findings (*SI Appendix*, Fig. S4 *C–E*). Under the longer incubation conditions, we observed competitive pharmacology, i.e., increase in K_m and no changes in V_{max}, in the presence of αPVP enantiomers and cocaine (control K_m = 2.6 μM, cocaine K_m = 7.2 μM, *S*-αPVP K_m = 4.8 μM, *R*-αPVP K_m = 3.4 μM, Fig. 3 *G–I*). In the case of *R*-αPVP, the K_m increase was not statistically significant.

We next examined the dissociation rate of inhibitors from DAT by taking advantage of the fast time-course (i.e., msec timescale) of DAT-mediated substrate-induced ionic currents. More specifically, we elicited DAT-mediated currents by applying a saturating concentration of dopamine (30 μM) to cells over-expressing the human DAT (white box). Once the steady-state DAT-mediated current was established, we co-applied the inhibitor of interest (yellow box) which reverses the current back to baseline, depending on its affinity for DAT and its ability to compete with dopamine binding at the orthosteric site (Fig. 3*B*). After a stable current reversal was established, application of the inhibitor is stopped and 30 μM dopamine is re-applied alone, restoring the current amplitude. The rate of recovery of the current is a measure of the k_{off} for the inhibitor being tested (right dashed box, Fig. 3*B*). As shown in the *Right Inset* of Fig. 3*B*, the dopamine-mediated current recovers in a concentration-independent manner as expected in the case of a k_{off} measure which is solely dependent on time (s^{-1}). In order to generalize our findings, we have therefore applied this protocol to an expanded number of psychostimulants and DAT inhibitors having either a pyrovalerone-related pharmacophore (*S*- and *R*-αPVP; *S*- and *R*-MDPV; *S*- and *R*-pyrovalerone) or a chemically distinct pharmacophore (i.e., cocaine, MPH, and ibogaine). The compounds were first tested in uptake inhibition assays to obtain their IC_{50} (*SI Appendix*, Fig. S5 *A–C*). To confirm a similar pharmacological profile as αPVP, we wished to rule out that a non-competitive profile is due to association with the allosteric binding site. Accordingly, the new compounds were added to COS-7 cells expressing hDAT and assessed whether they were able to inhibit the dissociation of the pre-bound high-affinity cocaine analogue [^{3}H]MFZ 2-12. If the compounds bound to the allosteric site, we would expect an impaired dissociation of [^{3}H]MFZ 2-12 as seen previously for S1-bound ligands in SERT (51, 56). As expected, none of the compounds could significantly impede the dissociation of [^{3}H]MFZ 2-12 (*SI Appendix*, Fig. S6).

As shown in Fig. 3*C*, we found heterogeneity in k_{off} values across the compounds. Nonlinear regression of the current-recovery slope provided an estimate of the respective k_{off} (Fig. 3*D* and *SI Appendix*, Table S3). DAT-mediated currents were re-established very quickly after washing out cocaine, ibogaine, *R*-MDPV, and *R*-pyrovalerone, whereas the DAT-mediated currents required a substantially longer time to re-establish (approximately 10-fold) in the case of *S*- and *R*-αPVP, *S*-MDPV, and *S*-pyrovalerone. MPH showed an intermediate effect. For representative recordings of each inhibitor, see *SI Appendix*, Fig. S5. Given that Kd = k_{off}/k_{on} and Kd generally reflects Ki, we suspect that DAT enantioselectivity of αPVP isomers is based on the different k_{on} values for each isomer, while in the case of MDPV and pyrovalerone enantiomers could be mediated by a mixed effect on both k_{on} and k_{off}. It was not possible to empirically determine the k_{on} due to the confounding effects introduced by the saturating concentration of dopamine necessary to elicit a reliable steady-state current. Indeed, dopamine is driving DAT through the entire transport cycle, including states in which the inhibitor cannot bind and therefore affecting drug k_{on}. These effects are not problematic in the case of the k_{off} determination.

To gain further information on the mechanism of interaction between the tested inhibitors and DAT, we have assessed the ability of each inhibitor to interact with one or more states of the transport cycle by measuring the respective maximal rate of DAT inhibition. The return step of the transporter (i.e., the "rate-limiting step"—Fig. 3*A*, dashed rectangle) is the slowest step of the transport cycle, therefore determining the overall maximal transport rate. Thus, for an inhibitor requiring a single state of the transporter for binding, the maximal rate of inhibition cannot supersede the rate-limiting step of the transporter (approximately 2 s^{-1}). However, in the case of compounds interacting with the transporter in more than one conformation (e.g., ibogaine), the rate constant for transporter inhibition (K_{app}) will supersede the rate-limiting step (57). In our electrophysiological recordings, we found that most of the compounds saturated at a rate consistent with the return step of DAT (1 to 2 s^{-1}) (58, 59), similar to cocaine and MPH. Interestingly, *R*-MDPV and *R*-pyrovalerone, at 100 μM, showed a similar maximal inhibition rate to ibogaine suggesting that they might access the transporter through different states of the transport cycle. As such, the analysis of DAT binding kinetics suggests that i) DAT inhibitors can differ in their k_{off}; ii) the non-competitive pharmacology might be due to slow binding kinetics; iii) the enantiomeric configuration of DAT inhibitors can shape both the k_{off} and/or their dependence on certain states of the transport cycle.

DAT Inhibitors Induce Stimulant Effects In Vivo that Reflect the In Vitro Enantioselective Binding Kinetics. Considering the heterogeneity in dissociation rates for DAT inhibitors, we wanted to evaluate if the enantioselective differences in the k_{off} values of DAT inhibitors might underlie the duration of their psychostimulant effects in vivo. Compound enantiomers possess

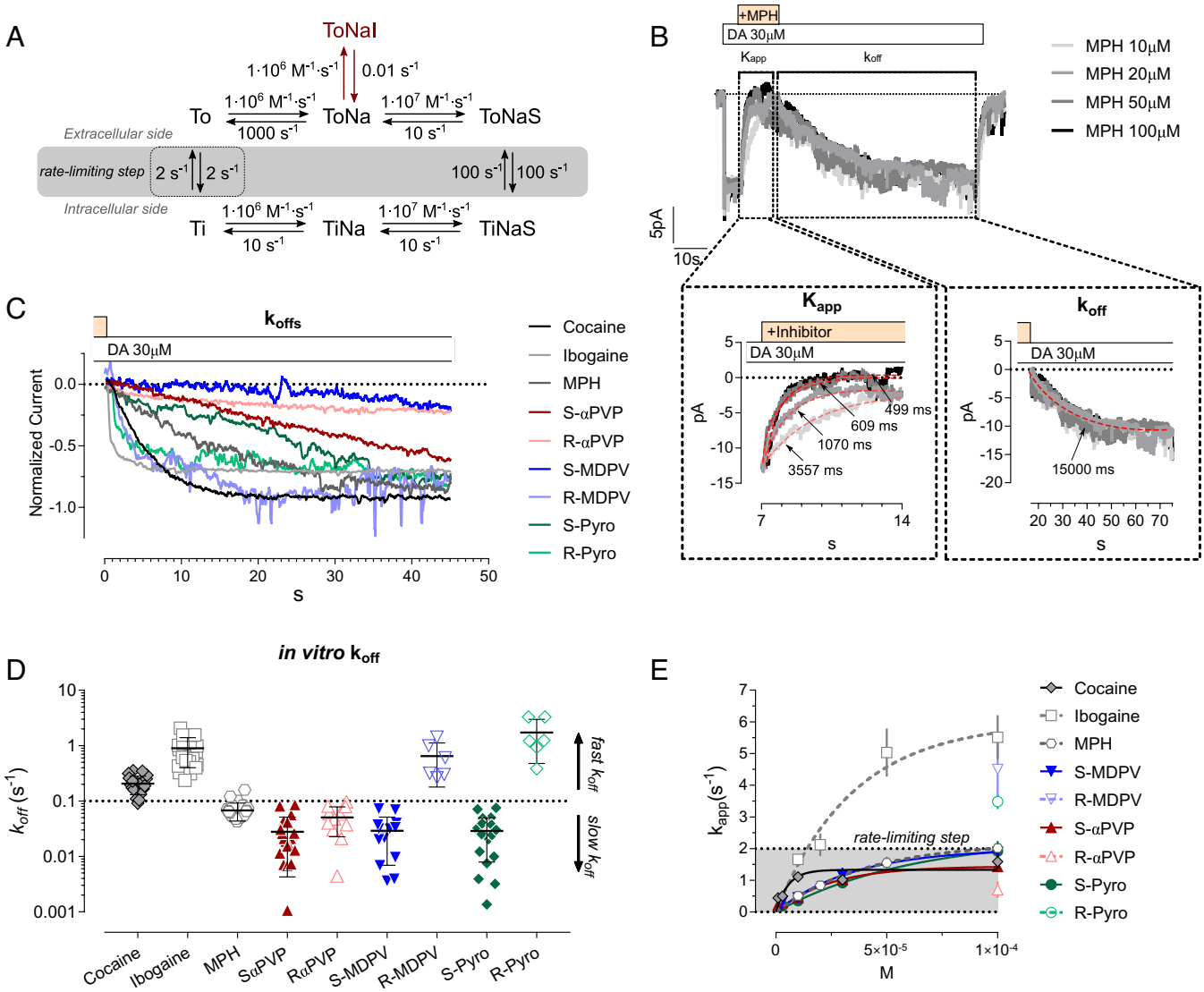

Fig. 3. Binding kinetics of cocaine and αPVP enantiomers at DAT. (*A*) Simplified DAT transport cycle used in the kinetic model with the kinetic rates for each partial reaction. The rate-limiting step is highlighted with the dashed rectangle and (*B*) representative trace and protocol employed for the measurement. DA application is highlighted by the white box, while the inhibitor application is highlighted by the yellow box. Dashed boxes indicate the part of the traces used for extrapolated the maximal inhibitory rate (K_{app}, *Left Inset*) or dissociation rates (k_{off}, *Right Inset*). Nonlinear regression fit of the different traces is represented with the red-dashed lines, together with the relative extrapolated decay time (*tau*; ms). (*C*) Corrected and normalized current rescue depicting the concentration-independent dissociation rates of the inhibitor. (*D*) Quantification of the dissociation rates of the tested DAT inhibitors. Data are mean ± SD. Each symbol represents an independent cell. (*E*) Representative trace of the synthetic currents obtained from the kinetic model. (*E*) Maximal rate of inhibition measured by extrapolating the time of current inhibition (K_{app}) at different concentrations of the tested inhibitor.

the same physicochemical properties (43). The DAT inhibitors tested also show similar predicted lipophilicity, as measured by LogP, to cocaine (cocaine = 3.08, MPH = 3.2, αPVP = 3.65, MDPV = 3.06, pyrovalerone = 4.11). Hence, we assumed that the time-course of psychostimulant effects on locomotor activity in WT C57Bl6/N mice might approximate binding kinetics of the tested DAT inhibitors. We tested the compounds in a simple time-course open field paradigm in mice (*SI Appendix*, Fig. S7). The cumulative distance traveled over 60 min post i.p. injection led to dose-response curves where *S*-αPVP, *S*-MDPV, and *S*-pyrovalerone were at least tenfold more potent than MPH, cocaine, *R*-αPVP, *R*-MDPV, and *R*-pyrovalerone (Fig. 4*A*), consistent with our in vitro uptake inhibition data (*SI Appendix*, Fig. S5 *A–C*). In addition, in order to extrapolate in vivo correlates of drug k_{off} at DAT (i.e., apparent dissociation rates), we defined the descending limb of the locomotor activity time-effect curve (i.e., 20 to 60 min post-injection) as an "in vivo apparent k_{off}" (*SI Appendix*, Fig. S8*A*). Evaluation of the descending limb of the time-course profile using linear regression showed no dose-dependency, as expected in the case of an in vivo correlate of k_{off} (see representative analysis in *SI Appendix*, Fig. S8*A*—*Right Insets*, and *SI Appendix*, Fig. S8 *B–D*). Consistent with the slow dissociation rates for αPVP enantiomers, *S*-MDPV, and pyrovalerone, the linear regression of the decline phase showed no dose-dependence or significance for the slopes of the enantiomers (*SI Appendix*, Table S4). Correlation analysis between the k_{off} measured in vitro and the in vivo extrapolated k_{off} led to a significant linear relationship (r^2 = 0.5827, P = 0.0275, F = 8.379). As represented in Fig. 4 *C–F* for all the tested DAT inhibitors, the duration of psychomotor stimulant effects was predicted by the binding kinetics observed in our in vitro experiments (cf. the dashed line in the *Left Inset* with the respective in vitro k_{off} on the *Right Inset*). Therefore, our findings support a key role for binding kinetics at DAT in discriminating between the "slow kinetics" inhibitors and the "fast kinetics" inhibitors.

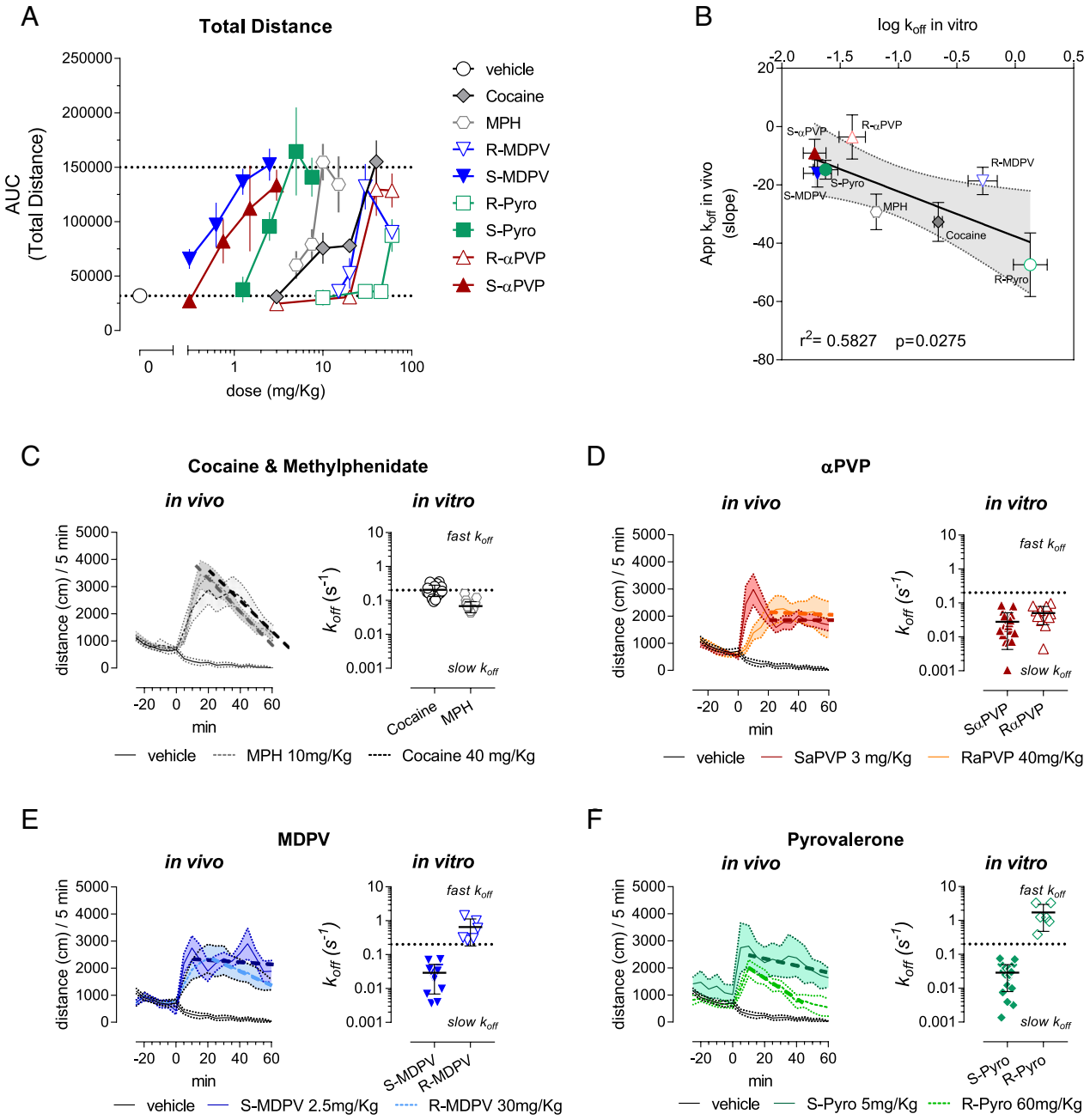

Fig. 4. DAT-mediated psychomotor effects in mice. (*A*) Dose-dependent effects of the DAT inhibitor tested in the total ambulatory distance measured over 60 min from i.p. injection. (*B*) Linear correlation between the apparent in vivo k_{off} and the log10 of the k_{off} measured in vitro. Linear regression led to a straight line with the equation Y = −15.43*X − 37.7; *P* =0.0275, F = 8.379, r^2 = 0.5827. (*C*–*F*) Comparison of the decline of action with the measured in vitro k_{off} for cocaine and MPH (*C*), S- and R-αPVP (*D*), S- and R-MDPV (*E*), S- and R-Pyrovalerone (*F*).

Discussion

Drugs which potently interact with DAT are historically associated with high abuse liability (11), especially those drugs which display higher potency at DAT in comparison with SERT (12, 13). Indeed, the preference for DAT over SERT, i.e., DAT/SERT selectivity ratio, is regularly used as a predictive indicator of the abuse liability of a given drug (14, 18). In agreement with previous studies (28), we found that *S*-αPVP has a high DAT/SERT selectivity ratio when compared to both cocaine and *R*-αPVP. However, despite the fact that DAT/SERT selectivity has been used as an index of abuse liability, several high affinity and DAT-selective inhibitors such as benztropines, rimcazole, GBR12909, and related analogs do not induce robust reinforcing and stimulatory effects (15, 60). On the other hand, cocaine, which clearly acts as a drug of abuse and also induces reinforcing and stimulatory effects, does not present with a high DAT/SERT selectivity ratio. Hence, the molecular basis for the differences in behavioral effects across different DAT inhibitors is still not completely understood, and numerous hypotheses have been put forward (15).

The in vitro pharmacology of drugs is normally assessed under thermodynamic equilibrium conditions, yet in the human body, the drug-target interactions are influenced by the constant flux of fluids and a variety of physiological processes. Hence, the in vitro effects of a given drug may not predict in vivo activity. In the past, it was suggested that the DAT-selective benztropine analog JHW007 can antagonize the reinforcing effects of cocaine by slowly occupying DAT in the CNS (61), indicating that binding

kinetics can influence behavioral properties of DAT ligands. Prior studies found that *S*-αPVP and *S*-MDPV engender robust self-administration in rats, while *R*-αPVP and *R*-MDPV are less potent in this regard (28, 62, 63), but a link with binding kinetics was not attempted. Establishing kinetic-activity relationships for DAT ligands may help to i) define the role of kinetics in pharmacological processes and ii) develop DAT inhibitors with reduced abuse liability.

In the present study, we compared the DAT binding kinetics of pyrovalerone analogs with more traditional DAT inhibitors like cocaine and MPH. In humans, αPVP and MDPV display a similar onset of action to cocaine but have longer-lasting effects, which may exacerbate their effects and consequently lead to serious intoxication (22, 24, 25, 27). Our systematic in vitro comparison of αPVP enantiomers and cocaine highlighted substantial differences between the kinetic profiles at DAT, which could be extended in vivo as significantly prolonged psychomotor effects of the αPVP enantiomers in mice. The relationship between slow k_{off} at DAT and sustained locomotor activity could be extended further to the structurally related drugs *S*-MDPV and *S*-pyrovalerone, therefore suggesting that the slow dissociation kinetics at DAT may underlie the long-lasting effects of these drugs.

Our in vitro experiments indicated that the slow dissociation kinetics of αPVP enantiomers are not related to the binding at an allosteric site on DAT, which differs from what is known about the allosteric SERT inhibitors *S*-citalopram (64, 65) and Lu AF60097 (52). Indeed, we found that αPVP enantiomers bind to the orthosteric site on DAT. However, when the F76 of DAT was mutated to the corresponding residue in SERT (DAT-F76Y), the potency of αPVP enantiomers in inhibiting dopamine uptake was reduced, while no changes were observed for cocaine. Thus, there are subtle differences between the binding of αPVP and cocaine to the orthosteric site on DAT. Our docking data agree with previous studies, where the F76 in DAT, together with the corresponding Y95 in SERT are key residues for substrate recognition in the central binding site (66–68).

Our computational data showed a slightly different interaction mode between DAT and *S*-αPVP compared to cocaine. While the aromatic ring of both drugs is located similarly to what has been reported in the case of dopamine, amphetamines, and inhibitors like cocaine, RTI-55, or nisoxetine structures (50, 69), *S*-αPVP protrudes deeper in the S1 binding site compared to cocaine, explaining why F76Y has an effect on *S*-αPVP but not on cocaine. The binding pose of αPVP is also consistent with the experimental data summarized in Fig. 2*G* for several reasons: i) The V152I mutant lowers the Ki of S-αPVP to DAT; ii) the binding pose suggests that the V152I mutation leads to an increase in hydrophobicity in the S1 site and therefore enhances the interaction with the aromatic moiety of *S*-αPVP; iii) mutations of S149 and S429 to alanine had minimal effects on Ki, which is in line with the binding pose showing no direct contacts of these residues with *S*-αPVP; iv) the mutation F76Y introduces an increase in local hydrophilicity at the bottom of the S1 binding site and an additional hydrogen bond donor which cannot be used by *S*-αPVP since the required rotation would perturb its interaction with the S1 site.

We show that the non-competitive pharmacology of αPVP is secondary to DAT binding kinetics since the non-competitive inhibition could be converted to a competitive profile by increasing incubation time for dopamine uptake. This pharmacological profile is consistent with a slow binding kinetics mechanism (53–55), and it is not due to DAT-internalization (*SI Appendix*, Fig. S3), similar to previous reports on cocaine (70, 71). Importantly, the slow binding kinetics mechanism of αPVP to DAT differs, at least in part, from the binding of the indole alkaloid ibogaine to SERT. Ibogaine exhibits a non-competitive pharmacology by stabilizing the inward-open conformation of SERT (57, 72, 73). For αPVP, similarly to ibogaine, we see non-competitive pharmacology without interactions with secondary sites. However, compared to ibogaine, αPVP seems to be more dependent on a single state of the transport cycle and shows a much slower k_{off}; similar results were obtained for *S*-MDPV and *S*-pyrovalerone. On the other hand, *R*-MDPV and *R*-pyrovalerone showed a similar profile to ibogaine suggesting that subtle differences in the chemical structure or the enantiomeric configuration of DAT inhibitors might drastically change their interaction mode with DAT. We could not rule out the final conformation stabilized by αPVP, but we may speculate that the binding of αPVP in the central binding site of DAT may elicit local structural re-arrangements that are preventing its dissociation. A similar mechanism has been recently shown in the case of the 5-HT2B receptor crystal structure in complex with lysergic acid diethylamide (74).

When examined in native tissue preparations, we observed differences in the relative potency of the various DAT ligands in HEK293 cells and synaptosomes, showing a rank order of potency of *S*-αPVP > cocaine > *R*-αPVP. By contrast, the rank order of drug potency in the FSCV slice experiments was *S*-αPVP > *R*-αPVP > cocaine. The differences in relative potency across the experiments could be related to the different assay preparations employed, where DAT sites are more readily accessible in uptake assays as compared to slice preparations where DAT sites are embedded in a complex cellular matrix. Other possibilities include non-DAT sites of action for PVP isomers, which contribute to their effects on dopamine clearance measured in the FSCV experiments.

Based on the collective in vitro studies, we examined whether the differences in binding kinetics between different DAT inhibitors could be reflected in their psychomotor stimulant properties in mice. By conducting time-course experiments, we compared the onset and decline of locomotor effects produced by the various drugs. We found that a slow k_{off} at DAT for *S*- and *R*-αPVP, *S*-MDPV, and *S*-pyrovalerone was associated with prolonged psychomotor effects of the drugs in vivo. Accordingly, the faster k_{off} for cocaine, MPH, *R*-MDPV, and *R*-pyrovalerone was associated with much shorter duration of locomotor effects. For all of the tested DAT inhibitors, the descending limb of the locomotor time-effect curve showed virtually no dose-dependence, as expected from an in vivo surrogate of k_{off}. By contrast, the onset of drug action always showed a clear dose-dependency, as expected from an in vivo surrogate of a k_{on}(*SI Appendix*, Fig. S7 and Table S4).

Collectively, our findings show that a prolonged residence time on DAT can have important repercussions: i) The in vivo stimulant effects of DAT inhibitors are prolonged, and ii) tightly bound drugs are not available for metabolic degradation.

It has been shown previously that the reinforcing effects mediated by αPVP both in monkeys and rats are substantially prolonged when compared to effects of cocaine (13, 75). Similarly, prolonged stimulatory effects have been observed for MDPV in experimental animals (76) and for pyrovalerone in controlled clinical studies in humans (21). The tested DAT inhibitors show striking differences in binding kinetics which strongly correlate with the decline of stimulant effects in vivo.

The slow off rate observed in the case of αPVP enantiomers, *S*-MDPV, and *S*-pyrovalerone at DAT has important consequences for understanding their serious and protracted side effects (at least for αPVP and MDPV) such as psychosis, delirium states, and cardiovascular complications (23, 31, 77). In this study, we have

focused on DAT because of its well -established role in psychomotor functions (4). However, considering the role of norepinephrine and NET in the regulation of blood pressure and heart rate (78), the structural similarities between DAT and NET (1), and the high affinity that αPVP, MDPV, and pyrovalerone have for NET (20), we surmise that a slow dissociation rate at NET might underlie the peripheral side effects commonly observed in drug users. A prolonged NET inhibition could dramatically impact the cardiovascular system due to the stimulatory role of norepinephrine in the regulation of blood pressure and heart rate (78). In agreement, administration of MDPV or αPVP-enantiomers in rats shows an extended increase in blood pressure (28, 79). However, it is important to consider that DAT, in addition to its important role in the brain, is also widely expressed peripherally (80). Prolonged inhibition of the peripheral DAT could therefore, in principle, result in a peripheral hyperdopaminergic state, consequently altering systemic blood pressure (81). A more systematic analysis focusing on the peripheral effects of DAT inhibitors will be required to further elucidate the molecular targets leading to possibly detrimental side effects.

In conclusion, we show that drug-binding kinetics at DAT can have a significant impact on the psychomotor stimulant effects of drugs in vivo. Given this information, a more detailed assessment of drug-binding kinetics for DAT inhibitors might provide insights for the design of novel compounds with improved clinical utility. Furthermore, our findings show how psychopharmacological research on illicit drugs may help to reach a better understanding of physiological and toxicological processes.

Materials and Methods

Uptake experiments were conducted to evaluate the competitive/non-competitive pharmacology of the inhibitors and to characterize DAT-mutants. Experiments were conducted in HEK293 cells as previously done (57, 82). Buffer was Krebs HEPES buffer, and radiotracers were 0.2 μM [^{3}H]DA for DAT and 0.2 μM [^{3}H]5-HT for SERT. Nonspecific uptake was determined in the presence of 30 μM MPH (DAT) or 10 μM paroxetine (SERT) and subtracted.

Binding experiments were used to evaluate the involvement of an S2-like site in DAT. Experiments were adapted from previous experiments (83). When conducted in membranes from HEK293 cells expressing DAT, we used 10 μg/assay of DAT membranes and [^{3}H]WIN35428 as a tracer. When conducted in whole cells instead, COS-7 expressing DAT were seeded onto poly-ornithine-coated plates and [^{3}H]MFZ 2-12 was used as a tracer.

Site-Directed Mutagenesis. QuikChange II site-directed mutagenesis kit (Agilent Technologies) was used to create DAT-mutants required for defining the interacting residues of DAT orthosteric site with the inhibitors.

Uptake inhibition experiments were conducted to assess the interaction of the inhibitors with WT and mutants of DAT as previously reported (82, 84). Conditions were the same as the uptake experiments described before. Uptake in the absence of the substance of interest was defined as 100% uptake.

Molecular Modeling. The mutagenesis data were integrated in a molecular model which highlights the interaction between the inhibitors and DAT. The homology model used is based on the outward-open crystal structure of hSERT [PDB ID: 5I71, (64)].

Confocal Microscopy. We used a YFP-tagged version of DAT and a Nikon laser scanning confocal microscope system to study DAT-internalization following inhibitor binding. Plasma membrane was stained with 0.4% Trypan blue (Sigma) for 5 min.

Kinetic modeling was performed as done previously (85). Systems Biology Toolbox and MATLAB 2015a (Mathworks) were used to study the time-dependent non-competitive pharmacology of the inhibitors.

Transporter electrophysiology was used to resolve the dissociation constant of the tested inhibitors in vitro and to assess the dependence of inhibitor binding on transporter state/s as reported previously (57, 86). Transporter-mediated current was recorded from HEK293 cells expressing DAT, in the whole-cell configuration. Cells were clamped at −60 mV and continuously superfused with the necessary solutions.

FSCV. FSCV in acute rat striatal slices was employed to test the reproducibility of the data in complex rodent systems. Acute slices were prepared from Long-Evans rats. 7 um carbon fibers were used for the recordings. Scans consisted of sweeps from −0.4 to 1.3 V and back to −0.4 V, at a rate of 400 V/s, and were obtained at 50 Hz. Dopamine release was electrically evoked every 90 s with a bipolar stimulating electrode and a single, constant current pulse (10 to 180 μA, 1 ms duration). All the procedures were carried out as done previously (87).

Behavioral Experiments. Procedures were adapted from previous experiments (88, 89). Open-field test in adult male WT C57Bl6/N mice (10 to 12 wk old at the beginning of the experiments) was used to derive correlates of in vivo binding kinetics. The compounds were freshly dissolved in saline the day of the experiments and injected i.p. The distance traveled during 90 min session was recorded in 5 min bins. All animals experiments were conducted in agreement with the ARRIVE guidelines and the UK Animals (Scientific Procedures Act, 1986 and associated guidelines, EU Directive 2010/63/EU for animal experiments) and approved by the national ethical committee on animal care and use (Bundesministerium für Bildung, Wissenschaft und Forschung: BMBWF-2022-0.121.471).

Detailed procedures and *Materials* used in the current study are provided in the *SI Appendix*.

Data, Materials, and Software Availability. Figures and tables data have been deposited in Figshare (https://doi.org/10.6084/m9.figshare.14958270.v1).

ACKNOWLEDGMENTS. We acknowledge Michael Freissmuth for data discussion and the NIDA drug supply program for supplying the enantiomers of αPVP and MDPV. This work was supported by the Austrian Science Fund/FWF, grant W1232 (MolTag to H.H.S.), grant P 33955-B (to H.H.S.), grant P 32017 (to T.S.), the Theodor Körner Fonds 2020 to J.M., and the Intramural Research Program of the National Institute on Drug Abuse, NIH, grant DA 000522-13 to M.H.B.

Author affiliations: [a]Center for Physiology and Pharmacology, Institute of Pharmacology, Medical University of Vienna, 1090 Vienna, Austria; [b]Center for Physiology and Pharmacology, Department of Neurophysiology and Neuropharmacology, Medical University of Vienna, 1090 Vienna, Austria; [c]Electrophysiology Research Section, National Institute on Drug Abuse, NIH, Baltimore, MD 21224; [d]Department of Neuroproteomics, Paracelsus Medical University, 5020 Salzburg, Austria; [e]Department of Neuroscience, Faculty of Health and Medical Sciences, University of Copenhagen, 2200 Copenhagen, Denmark; [f]Designer Drug Research Unit, Intramural Research Program, National Institute on Drug Abuse, NIH, Baltimore, MD 21224; and [g]AddRess, Center for Addiction Research and Science, Medical University of Vienna, 1090 Vienna, Austria

1. A. S. Kristensen *et al.*, SLC6 neurotransmitter transporters: Structure, function, and regulation. *Pharmacol. Rev.* **63**, 585–640 (2011), 10.1124/pr.108.000869.
2. J. E. Kilty, D. Lorang, S. G. Amara, Cloning and expression of a cocaine-sensitive rat dopamine transporter. *Science* **254**, 578–579 (1991), 10.1126/science.1948035.
3. S. Shimada *et al.*, Cloning and expression of a cocaine-sensitive dopamine transporter complementary DNA. *Science* **254**, 576–578 (1991), 10.1126/science.1948034.
4. B. Giros, M. Jaber, S. R. Jones, R. M. Wightman, M. G. Caron, Hyperlocomotion and indifference to cocaine and amphetamine in mice lacking the dopamine transporter. *Nature* **379**, 606–612 (1996), 10.1038/379606a0.
5. A. Penmatsa, K. H. Wang, E. Gouaux, X-ray structure of dopamine transporter elucidates antidepressant mechanism. *Nature* **503**, 85–90 (2013), 10.1038/nature12533.
6. D. Leo *et al.*, Pronounced hyperactivity, cognitive dysfunctions, and BDNF dysregulation in dopamine transporter knock-out rats. *J. Neurosci.* **38**, 1959–1972 (2018), 10.1523/JNEUROSCI.1931-17.2018.
7. M. S. Mazei-Robison *et al.*, Anomalous dopamine release associated with a human dopamine transporter coding variant. *J. Neurosci.* **28**, 7040–7046 (2008), 10.1523/JNEUROSCI.0473-08.2008.
8. F. H. Hansen *et al.*, Missense dopamine transporter mutations associate with adult parkinsonism and ADHD. *J. Clin. Invest.* **124**, 3107–3120 (2014), 10.1172/JCI73778.
9. S. Bhat, A. El-Kasaby, M. Freissmuth, S. Sucic, Functional and biochemical consequences of disease variants in neurotransmitter transporters: A special emphasis on folding and trafficking deficits. *Pharmacol. Ther.* **222**, 107785 (2021), 10.1016/j.pharmthera.2020.107785.

10. H. H. Sitte, M. Freissmuth, Amphetamines, new psychoactive drugs and the monoamine transporter cycle. *Trends Pharmacol. Sci.* **36**, 41–50 (2015), 10.1016/j.tips.2014.11.006.
11. M. C. Ritz, R. J. Lamb, S. R. Goldberg, M. J. Kuhar, Cocaine receptors on dopamine transporters are related to self-administration of cocaine. *Science* **237**, 1219–1223 (1987), 10.1126/science.2820058.
12. S. Wee *et al.*, Relationship between the serotonergic activity and reinforcing effects of a series of amphetamine analogs. *J. Pharmacol. Exp. Ther.* **313**, 848–854 (2005), 10.1124/jpet.104.080101.
13. B. M. Gannon *et al.*, The abuse-related effects of pyrrolidine-containing cathinones are related to their potency and selectivity to inhibit the dopamine transporter. *Neuropsychopharmacology* **43**, 2399–2407 (2018), 10.1038/s41386-018-0209-3.
14. C. Bauer, M. Banks, B. Blough, S. Negus, Use of intracranial self-stimulation to evaluate abuse-related and abuse-limiting effects of monoamine releasers in rats. *Br. J. Pharmacol.* **168**, 850–862 (2013), 10.1111/j.1476-5381.2012.02214.x.
15. M. E. A. Reith *et al.*, Behavioral, biological, and chemical perspectives on atypical agents targeting the dopamine transporter. *Drug Alcohol Depend.* **147**, 1–19 (2015), 10.1016/j.drugalcdep.2014.12.005.
16. R. B. Rothman, J. S. Partilla, M. H. Baumann, C. Lightfoot-Siordia, B. E. Blough, Studies of the biogenic amine transporters. 14. identification of low-efficacy "partial" substrates for the biogenic amine transporters. *J. Pharmacol. Exp. Ther.* **341**, 251–262 (2012), 10.1124/jpet.111.188946.
17. M. Niello, R. Gradisch, C. J. Loland, T. Stockner, H. H. Sitte, Allosteric modulation of neurotransmitter transporters as a therapeutic strategy. *Trends Pharmacol. Sci.* **41**, 446–463 (2020), 10.1016/j.tips.2020.04.006.
18. D. Luethi, M. E. Liechti, Designer drugs: Mechanism of action and adverse effects. *Arch. Toxicol.* **94**, 1085–1133 (2020), 10.1007/s00204-020-02693-7.
19. M. H. Baumann, H. M. Walters, M. Niello, H. H. Sitte, "Neuropharmacology of synthetic cathinones" in *Handbook of Experimental Pharmacology*, (Springer, New York LLC, 2018), pp. 113–142, 10.1007/164_2018_178.
20. P. C. Meltzer, D. Butler, J. R. Deschamps, B. K. Madras, 1-(4-Methylphenyl)-2-pyrrolidin-1-yl-pentan-1-one (pyrovalerone) analogues: A promising class of monoamine uptake inhibitors. *J. Med. Chem.* **49**, 1420–1432 (2006), 10.1021/jm050797a.
21. A. R. Holliday, R. B. Morris, R. P. Sharpley, Compound 84/F 1983 compared with D-amphetamine and placebo in regard to effects on human performance. *Psychopharmacologia* **6**, 192–200 (1964), 10.1007/BF00404009.
22. C. Crespi, Flakka-induced prolonged psychosis. *Case Rep. Psychiatry* **2016**, 1–2 (2016), 10.1155/2016/3460849.
23. L. Karila, G. Lafaye, A. Scocard, O. Cottencin, A. Benyamina, MDPV and α-PVP use in humans: The twisted sisters. *Neuropharmacology* **134**, 65–72 (2018), 10.1016/j.neuropharm.2017.10.007.
24. E. E. Richman *et al.*, α-pyrrolidinopentiophenone ("Flakka") Catalyzing catatonia: A case report and literature review. *J. Addict. Med.* **12**, 336–338 (2018), 10.1097/ADM.0000000000000407.
25. K. Romanek *et al.*, Synthetic cathinones in Southern Germany - characteristics of users, substance-patterns, co-ingestions, and complications. *Clin. Toxicol. (Phila)* **55**, 573–578 (2017), 10.1080/15563650.2017.1301463.
26. F. P. Mayer *et al.*, Phase I metabolites of mephedrone display biological activity as substrates at monoamine transporters. *Br. J. Pharmacol.* **173**, 2657–2668 (2016), 10.1111/bph.13547.
27. M. H. Baumann *et al.*, Neuropharmacology of 3,4-Methylenedioxypyrovalerone (MDPV), its metabolites, and related analogs. *Curr. Top. Behav. Neurosci.* **32**, 93–117 (2017), 10.1007/7854 _ 2016 _ 53.
28. C. W. Schindler *et al.*, Stereoselective neurochemical, behavioral, and cardiovascular effects of α-pyrrolidinovalerophenone enantiomers in male rats. *Addict. Biol.* **25**, e12842 (2020), 10.1111/adb.12842.
29. J. Maier *et al.*, α-PPP and its derivatives are selective partial releasers at the human norepinephrine transporter. *Neuropharmacology* **190**, 108570 (2021), 10.1016/j.neuropharm.2021.108570.
30. K. Kesha *et al.*, Methylenedioxypyrovalerone ("Bath Salts"), related death: Case report and review of the literature. *J. Forensic. Sci.* **58**, 1654–1659 (2013), 10.1111/1556-4029.12202.
31. J. Patocka *et al.*, Flakka: New dangerous synthetic cathinone on the drug scene. *Int. J. Mol. Sci.* **21**, 8185 (2020), 10.3390/ijms21218185.
32. R. Umebachi *et al.*, Clinical characteristics of α-pyrrolidinovalerophenone (α-PVP) poisoning. *Clin. Toxicol.* **54**, 563–567 (2016), 10.3109/15563650.2016.1166508.
33. T. Inaba, Cocaine: Pharmacokinetics and biotransformation in man. *Can. J. Physiol. Pharmacol.* **67**, 1154–1157 (1989), 10.1139/y89-184.
34. N. D. Volkow *et al.*, Is methylphenidate like cocaine?: Studies on their pharmacokinetics and distribution in the human brain. *Arch. Gen. Psychiatry* **52**, 456–463 (1995), 10.1001/archpsyc.1995.03950180042006.
35. J. S. Fowler, N. D. Volkow, G. J. Wang, S. J. Gatley, J. Logan, [11]Cocaine: PET studies of cocaine pharmacokinetics, dopamine transporter availability and dopamine transporter occupancy. *Nucl. Med. Biol.* **28**, 561–572 (2001), 10.1016/S0969-8051(01)00211-6.
36. J. M. Stogner, B. L. Miller, Investigating the 'bath salt' panic: The rarity of synthetic cathinone use among students in the United States. *Drug Alcohol Rev.* **32**, 545–549 (2013), 10.1111/DAR.12055.
37. J. J. Palamar, C. Rutherford, K. M. Keyes, "Flakka" use among high school seniors in the United States. *Drug Alcohol Depend.* **196**, 86–90 (2019), 10.1016/J.DRUGALCDEP.2018.12.014.
38. Y. Fujita *et al.*, Toxicokinetics of the synthetic cathinone α-pyrrolidinohexanophenone. *J. Anal. Toxicol.* **42**, e1–e5 (2018), 10.1093/JAT/BKX080.
39. M. Grapp, C. Kaufmann, H. M. Schwelm, M. A. Neukamm, Toxicological investigation of a case series involving the synthetic cathinone α-Pyrrolidinohexiophenone (α-PHP) and identification of phase I and II metabolites in human urine. *J. Anal. Toxicol.*, bkac057 (2022), 10.1093/JAT/BKAC057.
40. B. M. Gannon *et al.*, Relative reinforcing effects of second-generation synthetic cathinones: Acquisition of self-administration and fixed ratio dose-response curves in rats. *Neuropharmacology* **134**, 28–35 (2018), 10.1016/j.neuropharm.2017.08.018.
41. L. Duart-Castells *et al.*, Role of amino terminal substitutions in the pharmacological, rewarding and psychostimulant profiles of novel synthetic cathinones. *Neuropharmacology* **186**, 108475 (2021), 10.1016/j.neuropharm.2021.108475.
42. M. B. Gatch, S. B. Dolan, M. J. Forster, Comparative behavioral pharmacology of three pyrrolidine-containing synthetic cathinone derivatives. *J. Pharmacol. Exp. Ther.* **354**, 103–110 (2015), 10.1124/jpet.115.223586.
43. W. H. Brooks, W. C. Guida, K. G. Daniel, The significance of chirality in drug design and development. *Curr. Top. Med. Chem.* **11**, 760–770 (2011), 10.2174/156802611795165098.
44. R. A. Gregg *et al.*, Stereochemistry of mephedrone neuropharmacology: Enantiomer-specific behavioural and neurochemical effects in rats. *Br. J. Pharmacol.* **172**, 883–894 (2015), 10.1111/bph.12951.
45. H. L. Philogene-Khalid, C. Hicks, A. B. Reitz, L.-Y. Liu-Chen, S. M. Rawls, Synthetic cathinones and stereochemistry: S enantiomer of mephedrone reduces anxiety- and depressant-like effects in cocaine- or MDPV-abstinent rats. *Drug Alcohol Depend.* **178**, 119–125 (2017), 10.1016/j.drugalcdep.2017.04.024.
46. F. P. Mayer *et al.*, Stereochemistry of phase-1 metabolites of mephedrone determines their effectiveness as releasers at the serotonin transporter. *Neuropharmacology* **148**, 199–209 (2019), 10.1016/j.neuropharm.2018.12.032.
47. M. Niello *et al.*, Effects of hydroxylated mephedrone metabolites on monoamine transporter activity in vitro. *Front. Pharmacol.* **12**, 654061 (2021), 10.3389/fphar.2021.654061.
48. B. K. Krueger, Kinetics and block of dopamine uptake in synaptosomes from rat caudate nucleus. *J. Neurochem.* **55**, 260–267 (1990), 10.1111/j.1471-4159.1990.tb08847.x.
49. T. Beuming *et al.*, The binding sites for cocaine and dopamine in the dopamine transporter overlap. *Nat. Neurosci.* **11**, 780–789 (2008), 10.1038/nn.2146.
50. K. H. Wang, A. Penmatsa, E. Gouaux, Neurotransmitter and psychostimulant recognition by the dopamine transporter. *Nature* **521**, 322–327 (2015), 10.1038/nature14431.
51. P. Plenge *et al.*, The antidepressant drug vilazodone is an allosteric inhibitor of the serotonin transporter. *Nat. Commun.* **12**, 1–12 (2021), 10.1038/s41467-021-25363-3.
52. P. Plenge *et al.*, The mechanism of a high-affinity allosteric inhibitor of the serotonin transporter. *Nat. Commun.* **11**, 1491 (2020), 10.1038/s41467-020-15292-y.
53. H. P. Rang, The kinetics of action of acetylcholine antagonists in smooth muscle. *Proc. R. Soc. Lond. B. Biol. Sci.* **164**, 488–510 (1966), 10.1098/rspb.1966.0045.
54. T. Kenakin, Overview of receptor interactions of agonists and antagonists. *Curr. Protoc. Pharmacol.* (2008), 10.1002/0471141755.ph0401s42.
55. M. J. Lew, J. Ziogas, A. Christopoulos, Dynamic mechanisms of non-classical antagonism by competitive AT1 receptor antagonists. *Trends Pharmacol. Sci.* **21**, 376–381 (2000), 10.1016/S0165-6147(00)01523-6.
56. M. A. B. Larsen *et al.*, Structure-activity relationship studies of citalopram derivatives: Examining substituents conferring selectivity for the allosteric site in the 5-HT transporter. *Br. J. Pharmacol.* **173**, 925–936 (2016), 10.1111/bph.13411.
57. S. Bulling *et al.*, The mechanistic basis for noncompetitive ibogaine inhibition of serotonin and dopamine transporters. *J. Biol. Chem.* **287**, 18524–18534 (2012), 10.1074/jbc.M112.343681.
58. K. Erreger, C. Grewer, J. A. Javitch, A. Galli, Currents in response to rapid concentration jumps of amphetamine uncover novel aspects of human dopamine transporter function. *J. Neurosci.* **28**, 976–989 (2008), 10.1523/JNEUROSCI.2796-07.2008.
59. Y. Li *et al.*, Occupancy of the zinc-binding site by transition metals decreases the substrate affinity of the human dopamine transporter by an allosteric mechanism. *J. Biol. Chem.* **292**, 4235–4243 (2017), 10.1074/jbc.M116.760140.
60. A. H. Newman, S. Kulkarni, Probes for the dopamine transporter: New leads toward a cocaine-abuse therapeutic - A focus on analogues of benztropine and rimcazole. *Med. Res. Rev.* **22**, 429–464 (2002), 10.1002/med.10014.
61. R. I. Desai, T. A. Kopajtic, M. Koffarnus, A. H. Newman, J. L. Katz, Identification of a dopamine transporter ligand that blocks the stimulant effects of cocaine. *J. Neurosci.* **25**, 1889–1893 (2005), 10.1523/JNEUROSCI.4778-04.2005.
62. R. Kolanos *et al.*, Stereoselective actions of methylenedioxypyrovalerone (MDPV) to inhibit dopamine and norepinephrine transporters and facilitate intracranial self-stimulation in rats. *ACS Chem. Neurosci.* **6**, 771–777 (2015), 10.1021/ACSCHEMNEURO.5B00006.
63. B. M. Gannon, K. C. Rice, G. T. Collins, Reinforcing effects of abused "bath salts" constituents 3,4-methylenedioxypyrovalerone and α-pyrrolidinopentiophenone and their enantiomers. *Behav. Pharmacol.* **28**, 578–581 (2017), 10.1097/FBP.0000000000000315.
64. J. A. Coleman, E. M. Green, E. Gouaux, X-ray structures and mechanism of the human serotonin transporter. *Nature* **532**, 334–339 (2016), 10.1038/nature17629.
65. F. Chen, M. B. Larsen, C. Sánchez, O. Wiborg, The S-enantiomer of R, S-citalopram, increases inhibitor binding to the human serotonin transporter by an allosteric mechanism. Comparison with other serotonin transporter inhibitors. *Eur. Neuropsychopharmacol.* **15**, 193–198 (2005), 10.1016/j.euroneuro.2004.08.008.
66. M. B. Larsen *et al.*, Dopamine transport by the serotonin transporter: A mechanistically distinct mode of substrate translocation. *J. Neurosci.* **31**, 6605–6615 (2011), 10.1523/JNEUROSCI.0576-11.2011.
67. J. Grouleff, L. K. Ladefoged, H. Koldsø, B. Schiøtt, Monoamine transporters: Insights from molecular dynamics simulations. *Front. Pharmacol.* **6**, 235 (2015), 10.3389/fphar.2015.00235.
68. M. H. Cheng, I. Bahar, Monoamine transporters: Structure, intrinsic dynamics and allosteric regulation. *Nat. Struct. Mol. Biol.* **26**, 545–556 (2019), 10.1038/s41594-019-0253-7.
69. A. Penmatsa, K. H. Wang, E. Gouaux, X-ray structures of Drosophila dopamine transporter in complex with nisoxetine and reboxetine. *Nat. Struct. Mol. Biol.* **22**, 506–508 (2015), 10.1038/nsmb.3029.
70. K. Y. Little, L. W. Elmer, H. Zhong, J. O. Scheys, L. Zhang, Cocaine induction of dopamine transporter trafficking to the plasma membrane. *Mol. Pharmacol.* **61**, 436–445 (2002), 10.1124/MOL.61.2.436.
71. L. C. Daws *et al.*, Cocaine increases dopamine uptake and cell surface expression of dopamine transporters. *Biochem. Biophys. Res. Commun.* **290**, 1545–1550 (2002), 10.1006/bbrc.2002.6384.
72. M. T. Jacobs, Y. W. Zhang, S. D. Campbell, G. Rudnick, Ibogaine, a noncompetitive inhibitor of serotonin transport, acts by stabilizing the cytoplasm-facing state of the transporter. *J. Biol. Chem.* **282**, 29441–29447 (2007), 10.1074/jbc.M704456200.
73. J. A. Coleman *et al.*, Serotonin transporter–ibogaine complexes illuminate mechanisms of inhibition and transport. *Nature* **569**, 141–145 (2019), 10.1038/s41586-019-1135-1.
74. D. Wacker *et al.*, Crystal structure of an LSD-bound human serotonin receptor. *Cell* **168**, 377–389. e12 (2017), 10.1016/j.cell.2016.12.033.
75. G. T. Collins, A. Sulima, K. C. Rice, C. P. France, Self-administration of the synthetic cathinones 3,4-methylenedioxypyrovalerone (MDPV) and α-pyrrolidinopentiophenone (α-PVP) in rhesus monkeys. *Psychopharmacology (Berl)* **236**, 3677–3685 (2019), 10.1007/s00213-019-05339-4.
76. M. H. Baumann *et al.*, Powerful cocaine-like actions of 3,4-methylenedioxypyrovalerone (MDPV), a principal constituent of psychoactive "bath salts" products. *Neuropsychopharmacology* **38**, 552–562 (2013), 10.1038/npp.2012.204.
77. L. Nóbrega, R. J. Dinis-Oliveira, The synthetic cathinone α-pyrrolidinovalerophenone (α-PVP): Pharmacokinetic and pharmacodynamic clinical and forensic aspects. *Drug Metab. Rev.* **50**, 125–139 (2018), 10.1080/03602532.2018.1448867.

78. C. Schroeder, J. Jordan, Norepinephrine transporter function and human cardiovascular disease. *Am. J. Physiol. Hear. Circ. Physiol.* **303**, H1273-H1282 (2012), 10.1152/ajpheart.00492.2012.
79. C. W. Schindler, E. B. Thorndike, M. Suzuki, K. C. Rice, M. H. Baumann, Pharmacological mechanisms underlying the cardiovascular effects of the "bath salt" constituent 3,4-methylenedioxypyrovalerone (MDPV). *Br. J. Pharmacol.* **173**, 3492–3501 (2016), 10.1111/BPH.13640.
80. P. Mackie *et al.*, The dopamine transporter: An unrecognized nexus for dysfunctional peripheral immunity and signaling in Parkinson's Disease. *Brain Behav. Immun.* **70**, 21–35 (2018), 10.1016/j.bbi.2018.03.020.
81. R. C. Harris, M. Z. Zhang, Dopamine, the kidney, and hypertension. *Curr. Hypertens Rep.* **14**, 138–143 (2012), 10.1007/s11906-012-0253-z.
82. F. P. Mayer, Application of a combined approach to identify new psychoactive street drugs and decipher their mechanisms at monoamine transporters. *Curr. Top. Behav. Neurosci.* **32**, 333–350 (2016), 10.1007/7854_2016_63.
83. P. Plenge *et al.*, Steric hindrance mutagenesis in the conserved extracellular vestibule impedes allosteric binding of antidepressants to the serotonin transporter. *J. Biol. Chem.* **287**, 39316–39326 (2012), 10.1074/jbc.M112.371765.
84. M. Niello *et al.*, para-Trifluoromethyl-methcathinone is an allosteric modulator of the serotonin transporter. *Neuropharmacology* **161**, 107615 (2019), 10.1016/j.neuropharm.2019.04.021.
85. P. S. Hasenhuetl *et al.*, A kinetic account for amphetamine-induced monoamine release. *J. Gen. Physiol.* **150**, 431–451 (2018), 10.1085/jgp.201711915.
86. H. H. Sitte *et al.*, Carrier-mediated release, transport rates, and charge transfer induced by amphetamine, tyramine, and dopamine in mammalian cells transfected with the human dopamine transporter. *J. Neurochem.* **71**, 1289–1297 (1998), 10.1046/j.1471-4159.1998.71031289.x.
87. A. F. Hoffman, C. E. Spivak, C. R. Lupica, Enhanced dopamine release by dopamine transport inhibitors described by a restricted diffusion model and fast-scan cyclic voltammetry. *ACS Chem. Neurosci.* **7**, 700–709 (2016), 10.1021/acschemneuro.5b00277.
88. T. Steinkellner *et al.*, In vivo amphetamine action is contingent on αCaMKII. *Neuropsychopharmacology* **39**, 2681–2693 (2014), 10.1038/npp.2014.124.
89. S. Sideromenos *et al.*, The metabolic regulator USF-1 is involved in the control of affective behaviour in mice. *Transl. Psychiatry* **12**, 497 (2022), 10.1038/S41398-022-02266-5.